
# Attractive and repulsive interactions in the inelastic scattering of NO by Ar: A comparison between classical trajectory and close-coupling quantum mechanical results

F. J. Aoiz, J. E. Verdasco, V. J. Herrero, V. Sáez Rábanos, and M. A. Alexander

Citation: J. Chem. Phys. **119**, 5860 (2003); doi: 10.1063/1.1603223
View online: http://dx.doi.org/10.1063/1.1603223
View Table of Contents: http://jcp.aip.org/resource/1/JCPSA6/v119/i12
Published by the American Institute of Physics.

# Attractive and repulsive interactions in the inelastic scattering of NO by Ar: A comparison between classical trajectory and close-coupling quantum mechanical results

F. J. Aoiz[a] and J. E. Verdasco
*Departamento de Química Física, Facultad de Química, Universidad Complutense, 28040 Madrid, Spain*

V. J. Herrero
*Instituto de Estructura de la Materia (CSIC), Serrano 123, 28006 Madrid, Spain*

V. Sáez Rábanos
*Departamento de Química y Bioquímica, ETSI Montes, Universidad Politécnica, 28040, Madrid, Spain*

M. A. Alexander
*Department of Chemistry and Biochemistry and Institute for Physical Science and Technology, University of Maryland, College Park, Maryland 20742-2021*

(Received 4 June 2003; accepted 1 July 2003)

State-resolved differential cross sections for the rotationally inelastic scattering of the Ar+NO system have been derived from quasiclassical trajectories and quantum close-coupling calculations on a recent *ab initio* potential energy surface at the collision energy of a recent high resolution experiment (66 meV). Globally good agreement is obtained between the theoretical predictions and experimental results, although some of the experimental details are not reproduced in the classical calculation. The role of attractive and repulsive interactions in the observed dynamical features is examined. © *2003 American Institute of Physics.* [DOI: 10.1063/1.1603223]

## I. INTRODUCTION

The analysis of rainbow structures in the differential cross sections (DCSs) for atom–atom elastic scattering provides deep insight into the collision dynamics and valuable information on the underlying interatomic potentials.[1,2] The minimum in the interatomic potential gives rise to the classical rainbow singularity, which corresponds to a minimum (negative value) in the deflection angle as a function of the orbital angular momentum $L$ (or impact parameter $b$). In a quantum mechanical treatment, the singularity is removed. In addition, interference between different partial waves often gives rise to a number of secondary oscillations in the DCS.

In the 1970s, a series of systematic features observed in atom–molecule rotationally inelastic cross sections were classified as ''rainbows'' (see, for instance, Refs. 3, 4 and references therein). In inelastic collisions, the molecular anisotropy complicates the situation, even for the most simple case of two-dimensional atom–rigid rotor scattering. In general, the structure of the classical DCS will be determined by the mapping of $(L,\gamma)$ into $(\theta,j')$, where $\gamma$ is the initial orientation of the molecule with respect to the Jacobi center-of-mass separation vector $\mathbf{R}$, $\theta$ is the scattering angle in the center-of-mass frame, and $j'$ is the final rotational angular momentum of the molecule[5] (hereafter primed letters will refer to final state properties). Zeros in the Jacobian of this transformation will lead to the appearance of classical rainbow singularities.

The formal classification of these singularities is very complex.[3,5,6] However, under many circumstances, the dominant structures can be approximately divided into two types:[5,7,8] ''impact parameter'' or ''$L$-type'' rainbows, analogous to those found in elastic scattering, which are due to maxima in the deflection angle as a function of $L$, and ''orientational'' (or ''rotational'') rainbows caused by extrema in the final molecular angular momentum as a function of the orientation angle. Orientational rainbows can occur, even in the absence of a minimum in the potential. Most studies on rainbows in inelastic scattering have focused on this second type, characteristic of repulsive interactions and leading to high excitations (see, for instance, the references cited in Refs. 3,4).

The role of attractive forces in inelastic scattering has received less attention, although it was stressed in early model studies at thermal energies.[9,10] In more recent papers, Schinke *et al.*[5] and Mayne and Keil[8] used the infinite-order-sudden approximation (IOSA) and the quasiclassical trajectory (QCT) method to investigate the combined effects of attraction and repulsion on the characteristics of the DCSs for rotational excitation. These authors found that, depending on the potential shape, the collision energy, and the degree of rotational inelasticity, either $L$-type or orientational rainbows could dominate the inelastic DCSs. Inelastic collisions in Ar+HF, a system with a significant attractive well, were investigated experimentally and theoretically.[11,12] Although the main low-angle $L$-type rainbows were not resolved in the measurements, some of the features observed in the DCSs for individual final rotational levels were attributed to QM interference patterns between the attractive and repulsive parts of the potential.

[a]Author to whom correspondence should be addressed. Fax: +34 91394 4135; Electronic mail: aoiz@legendre.quim.ucm.es

 

Over the past two decades collisions of Ar with NO($X\,^2\Pi$) have been the subject of intense experimental[13–23] and theoretical[15,24–29] investigation. The open-shell character of the NO molecule has stimulated particular interest. As a result, this system has emerged a paradigm for the study of atom–molecule inelastic scattering. Several years ago, Alexander[28,29] reported coupled cluster [CCSD(T)] *ab initio* calculations of the two lowest Ar–NO adiabatic potential energy surfaces (PESs), designated $A'$ and $A''$ (which corresponds to the symmetry of the two lowest electronic states in $C_s$ symmetry). These two PESs arise when the electronic degeneracy of the ground ($X\,^2\Pi$) electronic state of NO is split by approach of the collision partner.

Based on the CCSD(T) PESs, full quantum close-coupling (CC) calculations of state-resolved rotationally inelastic DCS were carried out. These were found to be in excellent agreement with the most recent crossed-beam ion imaging experiments for both transitions in which the initial spin–orbit state ($\Omega=1/2$) is conserved as well as for transitions in which rotational excitation is accompanied by spin–orbit excitation ($\Omega=1/2\rightarrow3/2$).[22,23] Since rotational excitation from the ground ($j=0.5$) rotational level of NO up to $j'=15.5$ was investigated, the repulsive wall of the potential is clearly probed in these studies. However, since the nominal collision energy in the experiments (66 meV) is only roughly five times larger than the depth of the potential well,[28] and since the NO molecule has a small rotational constant ($B=1.7\,\mathrm{cm}^{-1}$), attractive interactions could also play an important role in excitation of the lower rotational states.

We describe here a combined QCT and CC QM investigation of rotational inelastic scattering of NO in collision with Ar at the collision energy of the experiments mentioned in the previous paragraph. Special attention has been paid to the dynamical origin of the various structures appearing in the rotationally state resolved DCSs. The study is limited to spin–orbit conserving collisions, which, in the Hund's case (a) limit, are governed by a single PES (which is the average of the $A'$ and $A''$ PESs, and designated $V_{\mathrm{sum}}$[30]). A classical treatment cannot account for multiplet changing processes, which are influenced by both PESs, although these processes can be treated approximately with surface-hopping trajectory methods.[31] The results of the present investigation are discussed and compared to the available experimental data.

## II. METHOD

The QCT calculation method is essentially the same as used in previous work.[32] We shall give only those specific details that are pertinent to the present study. A total number of $3.1\times10^5$ trajectories has been calculated on the $V_{\mathrm{sum}}$ PES of Alexander[28] for a collision energy ($E_{\mathrm{col}}$) of 532 $\mathrm{cm}^{-1}$ (66 meV) and with the NO molecule initially in its lowest rotational level. The $V_{\mathrm{sum}}$ PES, introduced in the preceding paragraph, governs rotational transitions within a given spin–orbit manifold ($\Delta\Omega=0$), and is defined as

$$V_{\mathrm{sum}}(R,\gamma)=\tfrac{1}{2}[V_{A''}(R,\gamma)+V_{A'}(R,\gamma)], \tag{1}$$

where $R$ and $\gamma$ have been defined in the Introduction. The indices $A'$ and $A''$ correspond to the two lowest CCSD(T) *ab initio* electronic states of the ArNO system.[28] Since the potential has been calculated only for NO held at its equilibrium internuclear distance, $r_e$, we use the method of Lagrange multipliers to force a rigid rotor constraint ($r=r_e$) in the integration of the classical equations of motion.[33,34] For the assignment of the final rotational quantum number, $j'$, the square of the classical angular momentum, $j'^2$ is equated to $j'(j'+1)/\hbar^2$. The values of $j'$ thus obtained are then rounded to the nearest integer. In the case of the first excited rotational state, only trajectories leading to $j'$ in the 1–1.5 range have been assigned to $j'=1$ in order to avoid a ''leaking'' of the elastic collisions, which are much more probable than inelastic events. This criterion is justified by a comparison with experiment and with QM calculations (see the next section).

To determine the value of the maximum impact parameter $b_{\mathrm{max}}$ used in the calculations, the change in rotational quantum number $\Delta j$ with an impact parameter was monitored. The impact parameter was increased until no trajectories leading to $\Delta j>0.5$ were found. With this procedure a value of 6.3 Å was derived for $b_{\mathrm{max}}$. The opacity functions and DCSs have been calculated by the method of moment expansion in Legendre polynomials.[32]

The full nonadiabatic quantum CC calculations were carried out with the HIBRIDON program suite,[36] as described in Refs. 22 and 29. To obtain convergence in the scattering calculations, all rotational levels with $j'\leqslant17.5$ have been used in the expansion of the scattering wave function. For each value of $j'$, both parity ($\lambda$) doublet levels and both spin–orbit levels $\Omega=1/2$ and 3/2 were included. Close-coupled calculations were carried out for all partial waves with $J_{\mathrm{tot}}\leqslant158.5$. This corresponds to a maximum impact parameter of $\approx6.8$ Å, which is comparable to the value needed for convergence in the QCT calculations.

Since the rotational levels of the NO molecule are half-integer, there arises an additional ambiguity in the comparison of the QM and QCT cross sections. In the QCT calculations we treat the NO molecule as a rigid rotor, with no internal (electronic orbital or spin) angular momenta. In our study here we assume that QCT cross sections for transitions from the lowest rotational level $j=0$ to the level $j'=j+\Delta j$ can be compared directly with the QM cross sections for transitions from the lowest rotational level $j=0.5$, $\Omega=1/2$ to the level $j'=0.5+\Delta j$, $\Omega=1/2$. In addition, since the QM transition for each $\Delta j$ corresponds to four distinct $\Lambda$-doublet resolved transitions ($e\rightarrow e$, $f\rightarrow f$, $e\rightarrow f$, and $f\rightarrow e$), we assume that the QCT cross section, $\sigma(\Delta j)$, should be compared with the sum (over the two final $\Lambda$-doublet levels) and average (over the two initial $\lambda$-doublet levels) of the QM cross sections. In other words,

$$\sigma_{\mathrm{QCT}}(\Delta j)\cong\frac{1}{2}\sum_{\varepsilon,\varepsilon'}\sigma_{\mathrm{QM}}(j,\varepsilon\rightarrow j',\varepsilon'), \tag{2}$$

where $\varepsilon=\pm1$ is the parity ($\Lambda$-doublet) index.

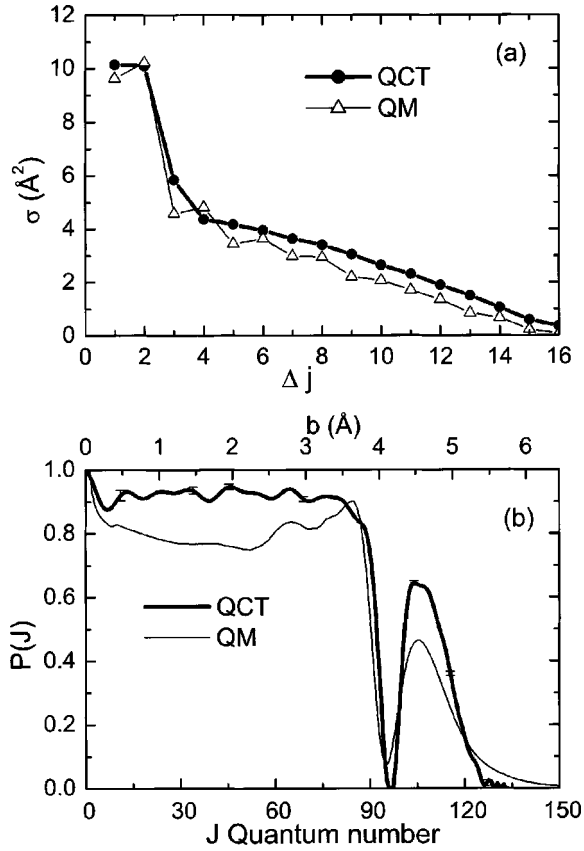


FIG. 1. (a) State-to-state integral cross section for the rotational excitation process $Ar+NO(\Omega=\frac{1}{2},j=0)\rightarrow Ar+NO(\Omega=\frac{1}{2},j+\Delta j)$. Closed circles and thick solid line, QCT results; open triangles and thin solid line close-coupling QM calculations. (b) Total opacity function for the spin-conserving ($\Delta\Omega=0$) rotational inelastic excitation of NO in its lowest rotational and spin–orbit state by Ar as a function of the total angular momentum quantum number, *J*, and impact parameter.

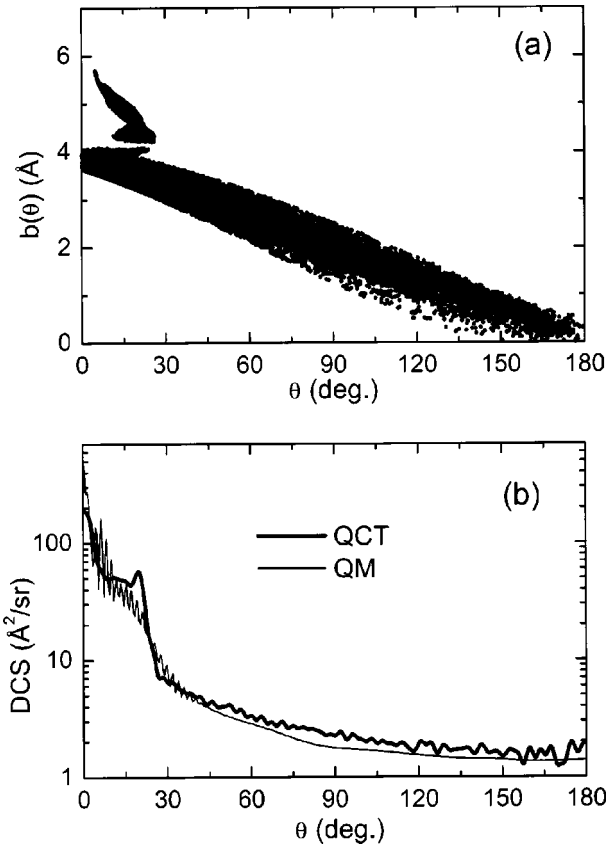


FIG. 2. (a) Classical deflection function for rotationally inelastic scattering of NO in its lowest rotational and spin–orbit state ($\Omega=\frac{1}{2},j=0$) by Ar. (b) Total, summed on all inelastic transitions, solid angle differential cross section for the same process.

## III. RESULTS AND DISCUSSION

Figure 1(a) shows a comparison between the QCT and QM integral cross sections for the various $\Delta j$ excitations of NO. Both calculations lead to a sudden drop in the cross section between $\Delta j=2$ and $\Delta j=3$ followed by a more gradual decrease with growing $\Delta j$. The probability of excitation of rotational states with $\Delta j\geqslant 16$ is negligible at the collision energy considered. For $\Delta j\geqslant 5$, the QCT cross sections are systematically slightly larger than the QM values. As indicated in the previous section, the QCT cross section for $\Delta j=1$ is very sensitive to the binning procedure employed for the assignment of the final quantum states. With the criterion adopted, the classical cross section is in good agreement with the QM result and with the value measured by Joswig *et al.*[15] for a somewhat lower collision energy (55.5 meV). If trajectories leading to $0.5<j'<1$ are also assigned to $j'=1$, the QCT cross section for $\Delta j=1$ is increased by a factor of about 3. Although our chosen criterion may lead to an underestimation of $\sigma(\Delta j=1)$, it ensures that all the dynamical effects discussed below apply to rotationally inelastic processes.

The quantum CC integral cross sections show oscillations as a function of $\Delta j$ that are not reproduced in the classical calculations. This oscillatory structure, more pronounced at low $\Delta j$, was previously found in the experimental results of Joswig *et al.*[15] at 55.5 meV collision energy, and it was reproduced by coupled state calculations presented in the same work. As discussed by Joswig *et al.*, these oscillations are the effect of a semiclassical interference due to the near-homonuclear character of the NO molecule, first analyzed by Miller and McCurdy.[35]

The total opacity function, $P(J)$, for inelastic scattering (obtained by summing over all the inelastic excitations) is shown in Fig. 1(b). The classical excitation probability is close to 0.9 for values of the impact parameter between 0 and $\approx 3.7$ Å ($J=90$), and then drops quickly to zero at about $b=4.2$ Å ($J=95$). For a narrow range of impact parameters (orbital angular momenta) around this value, no rotational excitation is possible at the collision energy considered. For higher impact parameters the opacity function has another lobe extending up to $b\approx 6$ Å ($J=140$). The quantum mechanical $P(J)$ is very similar in shape, but is consistently a bit smaller and extends to slightly larger values of the angular momentum.

The two lobes in the opacity function correspond to two dynamical regimes. This is clearly illustrated in Fig. 2, where the total (summed on all $\Delta j>0$ transitions) QM and QCT inelastic DCS and the classical deflection function, $b(\theta)$, are shown in the lower and upper panel, respectively. The good agreement between the QM and QCT DCS is worth noting. At first sight, the results displayed are reminiscent of the

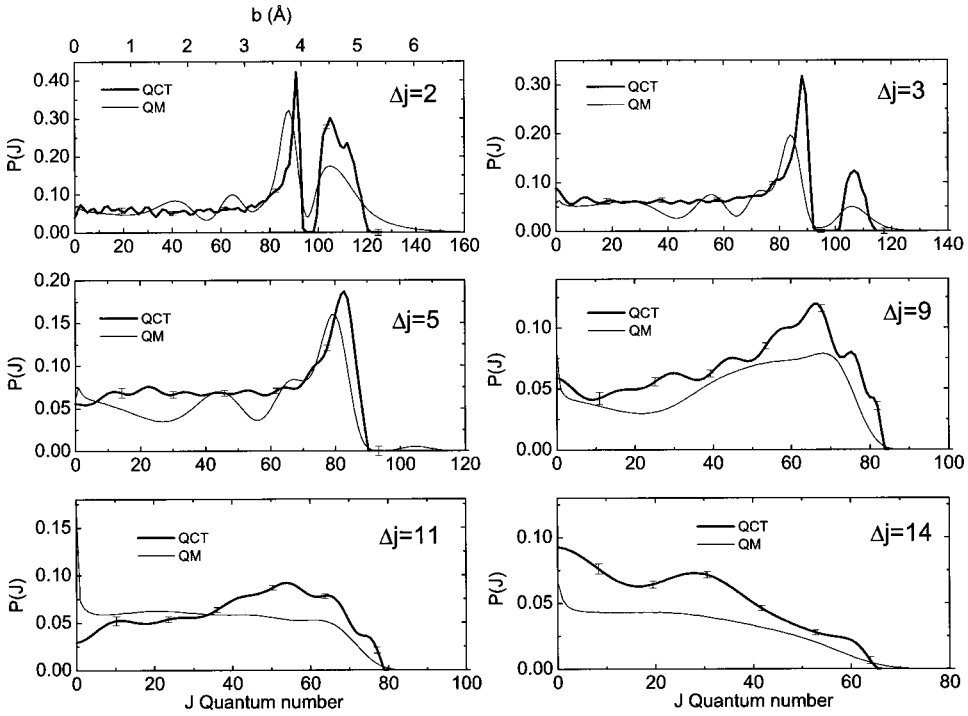


FIG. 3. QCT and QM opacity functions for rotational excitation from the lowest rotational state of NO in the $\Omega=1/2$ spin–orbit manifold. The CC QM results have been summed over final $\Lambda$-doublet levels and averaged over the $\Lambda$-doublet levels of the initial rotational state.

classical elastic scattering of structureless particles by a spherical potential, but, as expected, this picture is blurred by the anisotropy of the actual Ar–NO potential that leads to a damping of the main rainbow feature, appearing at $\theta_r \approx 20°$, and disperses the outcome of the classical trajectories into a band of $(b,\theta)$ values lying around the curve that would correspond to elastic scattering.

The results illustrated in Fig. 2 are typical of inelastic scattering in the presence of a significant attractive well, as discussed by Schinke *et al.*[5] and by Mayne and Keil[8] in their theoretical studies of model systems. The concentration of trajectories with different impact parameters giving rise to the classical rainbow and the crucial, but not exclusive, contribution of attractive trajectories to this DCS feature are clearly discernible in this figure. This *L*-type (attractive) rainbow[5,8] divides the DCS into a ''bright'' component for angles lower than $\theta_r$ and a ''dark'' component for angles larger than $\theta_r$, where the probability of scattering is much lower.

Note that the dip observed in the total opacity function $P(J)$ [Fig. 1(b)], which is mirrored by a discontinuity in the calculated deflection function, occurs over a narrow range of impact parameters very close to the location of the transition between attractive deflection, characterized by the familiar high impact parameter bulge in $b(\theta)$, and repulsive deflection, manifest in the other branch of the deflection function, which shows the increase in scattering angle with decreasing *b*. A perfect compensation between attraction and repulsion would result in undeflected classical trajectories (glory scattering), and would also preclude the appearance of inelastic excitation given the absence of a mechanism for the transfer of energy and angular momentum between the collision partners. Although the glory singularity is smeared in the trajectory calculations by the already mentioned anisotropy of the potential, there is a small range of impact parameters, where the effects of the attractive and repulsive forces are nearly balanced so that rotational excitation does not occur. A qualitatively similar opacity function, with a minimum for an intermediate range of impact parameters, was obtained by Barnett and Mayne[12] in a semiclassical calculation of the Ar $+\mathrm{HF}(j=0)\rightarrow\mathrm{Ar}+\mathrm{HF}(j'=1)$ process. Interestingly, these authors did not find a minimum in the corresponding classical $P(J)$ and therefore concluded that this minimum was a quantum effect. In contrast, the present results suggest strongly that the possible appearance of minima in $P(J)$ caused by a near cancellation of attractive and repulsive interactions is well accounted for in a classical description.

To explore in more detail the origin and implications of the observed cleft between the two lobes of the total opacity function, it is worthwhile to investigate the inelastic scattering into individual final rotational levels. Classical and quantum mechanical opacity functions for the excitation of selected rotational levels are displayed in Fig. 3. As for the total opacity function, we observe excellent good global agreement between the predictions of the two theoretical methods. As can be seen, twin lobes in the opacity functions appear only for transitions with small rotational inelasticity ($\Delta j$ small). In the QCT calculations the high-*b* lobe appears only for $\Delta j \leqslant 3$; in the QM calculations, the excitation probability for low $\Delta j$ extends to higher *b* values and a very small high-*b* lobe appears, even for $\Delta j=5$. For larger $\Delta j$ values, the high-*b* ''attractive'' lobe in $P(b)$ disappears since the relatively weak interactions at a large impact parameter cannot impart the large torques needed for high degrees of rotational excitations.

The similarity in the shapes of the QM and QCT $\Delta j$-resolved opacity functions is reflected, as might be anticipated, in the corresponding DCSs, which are displayed in Fig. 4. For the lower values of $\Delta j$, the angular distributions

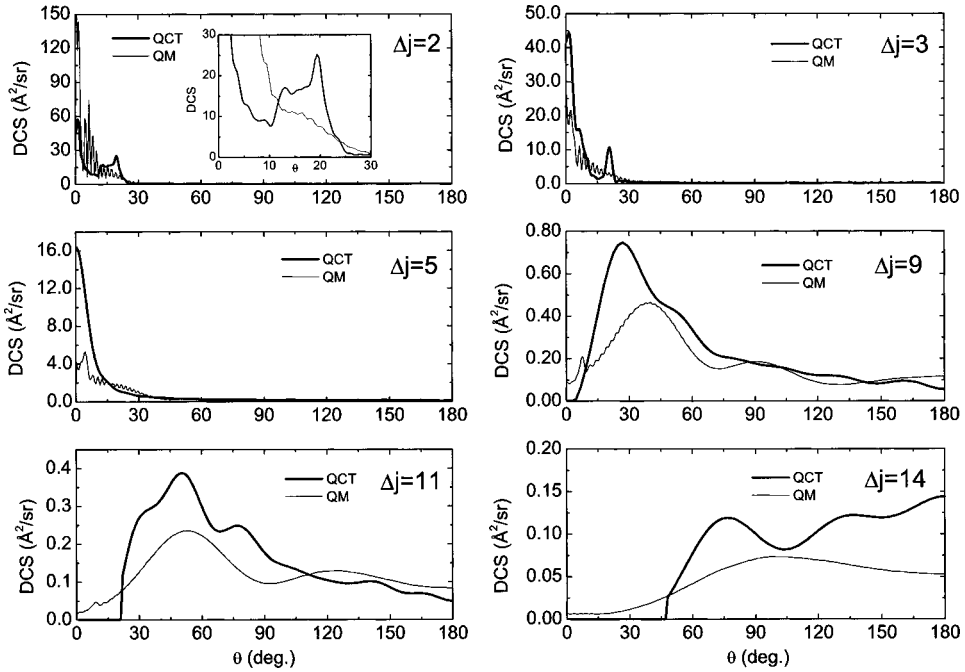


FIG. 4. QCT and QM state-resolved inelastic DCSs for rotational excitation from the lowest rotational state of NO in the $\Omega=1/2$ spin–orbit manifold. The CC QM DCSs have been summed over final $\Lambda$-doublet levels and averaged over the $\Lambda$-doublet levels of the initial rotational state. In the inset of the upper left panel, the fast QM oscillations have been smoothed to allow a more meaningful comparison of the broader features with the classical DCS.

are concentrated in the forward region, but shift gradually to backward angles with growing inelastic excitation. For $\Delta j=2$ and 3, the QM DCSs show pronounced fast oscillations, caused by interferences between the high number of partial waves that contribute for inelastic transitions with these small values of $\Delta j$. For $\Delta j=2$ the classical DCS has a secondary maximum at about 20°. An inspection of Figs. 2(b) and 3 shows that the contribution of attractive interactions leading to $\Delta j=2$ excitations is concentrated in the angular range of this maximum, which constitutes a marked *L*-type rainbow. The analysis of the DCS indicates that this maximum is almost exclusively caused by trajectories pertaining to the high *b* ''attractive'' bulge shown in Fig. 3.

Since the cross section is proportional to the integral over *b* of $P(b)$ multiplied by *b* [or, quantum mechanically, the sum over *J* of $(2J+1)P(J)$], one concludes that most of the $\Delta j=2$ inelastic flux (more than 50% of the trajectories) is influenced by attractive excitations. The preponderance of attractive scattering around 20° would be readily discernible in the corresponding polar DCS (not shown), which is weighted by $\sin\theta$. In the QM calculation this rainbow feature is smoothed and appears only as a shoulder, as shown in the inset in the upper left hand panel in Fig. 4.

For $\Delta j=3$ transitions, both the magnitude of the QM fast oscillations and the contribution of attractive scattering (centered now at about 25°) are smaller compared to the scattering at lower angles. This decrease in the importance of the attractive (large *b*) mechanism for inelastic excitation is responsible for the marked drop in the integral inelastic cross section between $\Delta j=2$ and $\Delta j=3$ [see Fig. 1(a) of this article and Fig. 5 of Ref. 15). Scattering corresponding to $\Delta j=5$ is already dominated by repulsive forces. In fact, the analysis of the trajectory calculations clearly indicates that the contribution of attractive interactions, which gives rise to the second lobe in the opacity functions, is almost negligible. Forward scattering of the excited molecules, which in this case is due to repulsion leading to small (positive) deflections is still noticeable, but the inelastic flux into large scattering angles begins to prevail. This may not be apparent from a first inspection of the solid angle (i.e., not weighted by $\sin\theta$) DCS of Fig. 4; nevertheless, the integration of the DCS shows that the partial cross section into the 0°–30° angular range is 43% and 41.9% of the $\Delta j=5$ total cross sections in the QM and QCT calculations, respectively. Therefore, the total flux into angles >30° is larger than that in the forward direction. More impulsive collisions are necessary to cause increasing rotational excitation. Consequently, the scattering becomes more backward peaked. As a result, the DCSs shown in Fig. 4 for $\Delta j=9$, 11, and 14 exhibit a characteristic structure dominated by orientational rainbows,[3,5,8] which shift to larger angles with an increasing degree of excitation.

Orientational rainbows rise fairly abruptly from the low angle side and then decline more slowly toward backward angles. In other words, the ''dark'' side of the rainbow corresponds to small angles and the ''bright'' side, to larger angles. In the classical case the low angle region (dark side) is forbidden. In the QM calculations, smooth oscillations corresponding to secondary orientational rainbows[3] are also observed, as can be clearly seen in the figure for $\Delta j=9$. These broad, regular oscillations are absent from the QCT results (the smallest undulations appearing in some of the QCT DCSs displayed in Fig. 4 are within the statistical uncertainties in the expansion of the DCSs in Legendre polynomials[32]). The narrow QM oscillations disappear gradually with growing $\Delta j$ due to the decrease in the number of partial waves, which lead to excitation of the high $j'$ states.

A comparison of the present QCT and the experimental DCSs of Kohguchi *et al.*[22] is shown in Fig. 5 (the corresponding comparison with the QM results for these rotational levels was presented in Ref. 22.) Unfortunately, the

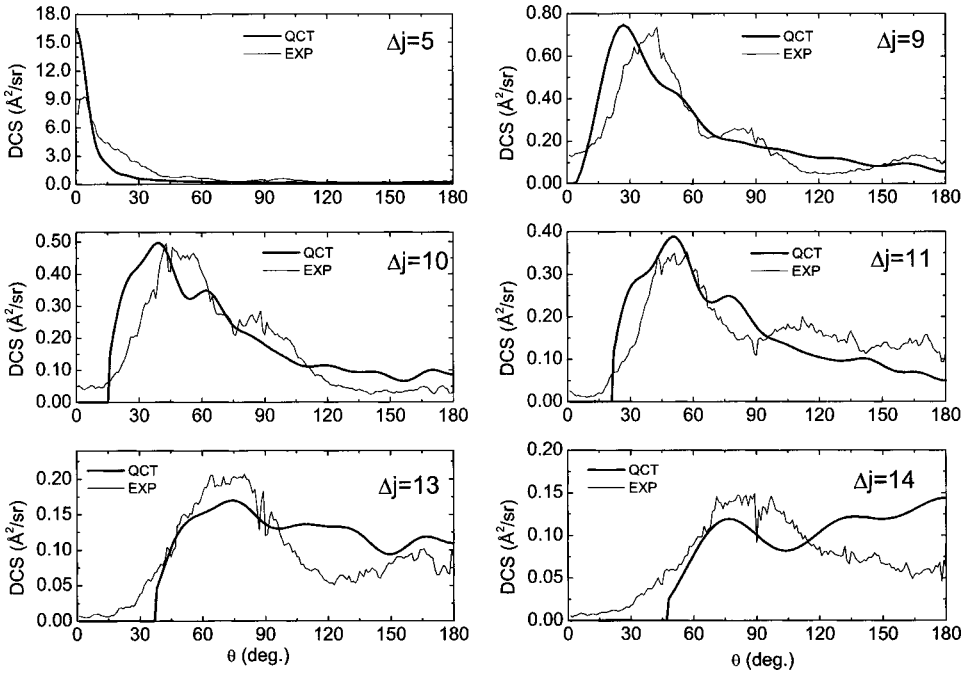


FIG. 5. A comparison of experimental (Ref. 22) and QCT state-resolved inelastic differential cross sections for the excitation of NO in its ground spin–orbit and rotational states by collision with Ar. A least squares fit was used to scale the experimental results to the theoretical values.

experiments did not yield absolute values of the DCSs. Consequently, in the comparison we scaled the experimental results to the theoretical DCS using a least square minimization of the deviations. The general evolution from forward to backward scattering with increasing $\Delta j$ described in the previous paragraph agrees with the experimental observations. The agreement between the experimental and QCT DCSs for individual $j'$ values is reasonably good, although some of the details, such as the broad, smooth oscillations corresponding to secondary rainbows discussed in the preceding paragraphs, are not reproduced in the QCT simulations. Unfortunately, due likely to the presence of low-lying excited rotational levels in the initial beam, experimental DCSs for excitation of the lowest $j'$ levels in the $\Omega=1/2$ spin–orbit manifold, were not reported.[22]

## IV. SUMMARY AND CONCLUSIONS

A detailed classical and quantum mechanical study of rotationally inelastic scattering of NO by Ar has been carried out at the collision energy of a recent high resolution experiment. State-resolved integral and differential cross sections were calculated for all the excited levels of NO in the lowest spin–orbit manifold. Repulsive interactions were seen to be similarly responsible for the excitation of rotational levels with $\Delta j \geqslant 5$. The corresponding differential cross sections are dominated by rotational rainbows that shift to increasingly backward angles with an increasing degree of rotational excitation. The quasiclassical trajectory approach can reproduce satisfactorily the overall shapes and trends seen in both the experimental and quantum mechanical state-resolved differential cross sections, but fails to account for the fast oscillations and secondary rainbows caused by quantum mechanical interferences.

At the comparatively low collision energy considered, both attraction and repulsion were found to contribute to inelastic excitation of the lowest rotational states. In fact, for $\Delta j \leqslant 3$, attraction is the dominant excitation mechanism. Overall, attractive interactions are responsible for about 22% of the inelastic trajectories. The differential cross sections for transitions with $\Delta j \leqslant 3$ show prominent impact parameter rainbows for center-of-mass scattering angles close to 20°. In the quantum calculations, this rainbow feature is appreciably smoothed, as might be expected. Unfortunately no experimental differential cross sections were reported for scattering into these low-lying rotational states.

Both the classical and the quantum mechanical treatment predict the existence of a small range of impact parameters over which rotational excitation does not occur. Here, the effects of attractive and repulsive interactions cancel each other out, with the result that a pronounced minimum occurs in the opacity function. This feature, which appears only for transitions with small $\Delta j$, provides a clear-cut separation between the attractive and repulsive dynamical regimes for rotational excitation. The abrupt disappearance of the attractive (large impact parameter) excitation mechanism as $\Delta j$ increases leads to a marked drop in the calculated values of the QCT and QM integral cross sections between $\Delta j=2$ and $\Delta j=3$, in agreement with previous experimental observations.

The good agreement between the QM and QCT differential and integral cross sections reveals that the essential details of the spin–orbit conserving transitions of NO in collisions with Ar are fully retained in the QCT simulations. Additionally, the QCT calculations provide more direct insight into the interplay between the forces that lead to rotational excitation of this diatomic molecule.

## ACKNOWLEDGMENTS

This work has been funded by the Ministry of Science and Technology of Spain under Grants No. BQU2002-04627-C02 and No. REN 2000-1557, by the European Union through the RTN Reaction Dynamics (HPRN-CT-1999-

0007), and by the U.S. National Science Foundation (Grant No. CHE-9971810) The research was performed within the Unidad Asociada ''Química Física Molecular'' between the Universidad Complutense and the CSIC.

[1] R. D. Levine and R. B. Bernstein, *Molecular Reaction Dynamics and Chemical Reactivity* (Oxford University Press, Oxford, 1987).
[2] U. Buck, in *Atomic and Molecular Beam Methods*, edited by G. Scoles (Oxford University Press, New York, 1988), Vol. 1, p. 499, and references therein.
[3] R. Schinke and J. M. Bowman, in *Molecular Collision Dynamics*, edited by J. M. Bowman (Springer-Verlag, Heidelberg, 1983), p. 61.
[4] U. Buck, in *Atomic and Molecular Beam Methods*, edited by G. Scoles (Oxford University Press, New York, 1988), Vol. 1, p. 525.
[5] R. Schinke, H.-J. Korsch, and D. Poppe, J. Chem. Phys. **77**, 6005 (1982).
[6] L. D. Thomas, J. Chem. Phys. **74**, 5905 (1980).
[7] L. D. Thomas, J. Chem. Phys. **67**, 5224 (1977).
[8] H. R. Mayne and M. Keil, J. Phys. Chem. **88**, 883 (1984).
[9] R. B. Bernstein and K. H. Kramer, J. Chem. Phys. **44**, 4473 (1966).
[10] R. W. Fenstermaker and R. B. Bernstein, J. Chem. Phys. **47**, 4417 (1967).
[11] L. J. Rawluk, M. Keil, M. H. Alexander, H. R. Mayne, and J. J. C. Barett, Chem. Phys. Lett. **202**, 291 (1993).
[12] J. J. C. Barrett and H. R. Mayne, J. Chem. Phys. **100**, 304 (1994).
[13] H. Thuis, S. Stolte, and J. Reuss, Chem. Phys. **43**, 351 (1979).
[14] P. Casavecchia, A. Laganà, and G. G. Volpi, Chem. Phys. Lett. **112**, 445 (1984).
[15] H. Joswig, P. Andresen, and R. Schinke, J. Chem. Phys. **85**, 1904 (1986).
[16] L. S. Bontuyan, A. G. Suits, P. L. Houston, and B. J. Whitaker, J. Phys. Chem. **97**, 6342 (1993).
[17] S. Jons, J. E. Shirley, M. T. Vonk, C. F. Giese, and W. R. Gentry, J. Chem. Phys. **105**, 5397 (1996).
[18] C. R. Bieler, A. Sanov, and H. Reisler, Chem. Phys. Lett. **175**, 235 (1995).
[19] A. Lin, S. Antonova, A. P. Tsakotellis, and G. C. McBane, J. Phys. Chem. A **103**, 1198 (1999).
[20] A. A. Dixit, P. J. Pisano, and P. L. Houston, J. Phys. Chem. A **105**, 11165 (2001).
[21] K. T. Lorenz, D. W. Chandler, J. W. Barr, W. Chen, G. L. Barnes, and J. I. Cline, Science **293**, 2063 (2001).
[22] H. Kohguchi, T. Suzuki, and M. Alexander, Science **294**, 832 (2001).
[23] M. S. Elioff and D. W. Chandler, J. Chem. Phys. **117**, 6455 (2002).
[24] G. C. Nielson, G. A. Parker, and R. T Pack, J. Chem. Phys. **66**, 1396 (1977).
[25] M. H. Alexander, Chem. Phys. **92**, 337 (1985).
[26] G. C. Corey and M. H. Alexander, J. Chem. Phys. **85**, 5652 (1986).
[27] M. H. Alexander, J. Chem. Phys. **99**, 7725 (1993).
[28] M. H. Alexander, J. Chem. Phys. **111**, 7426 (1999).
[29] M. H. Alexander, J. Chem. Phys. **111**, 7435 (1999).
[30] M. H. Alexander, J. Chem. Phys. **76**, 5974 (1982).
[31] G. Parlant and M. H. Alexander, J. Chem. Phys. **92**, 2287 (1990).
[32] F. J. Aoiz, V. J. Herrero, and V. Sáez Rábanos, J. Chem. Phys. **97**, 7423 (1992).
[33] R. A. LaBudde and R. B. Bernstein, J. Chem. Phys. **55**, 5499 (1971).
[34] M. D. Pattengill, in *Atom Molecule Collision Theory*, edited by R. B. Bernstein (Plenum, New York, 1979), p. 359.
[35] C. W. McCurdy and W. H. Miller, J. Chem. Phys. **67**, 463 (1977).
[36] HIBRIDON is a program package for the time-independent quantum treatment of inelastic collisions and photodissociation written by M. H. Alexander, D. E. Manolopoulos, H.-J. Werner, and B. Follmeg, with contributions by P. F. Vohralik, D. Lemoine, G. Corey *et al.* More information and a copy of the code can be obtained from the web site: http//www.chem.umd.edu/physical/alexander/hibridon